

EFFECTS OF PROPELLER LOCATIONS ON THE VORTEX SYSTEM ABOVE DELTA-SHAPED UAV MODEL

Khushairi Amri Kasim, Shabudin Mat, Iskandar Shah Ishak, Mazuriah Said
Faculty of Mechanical Engineering, Universiti Teknologi Malaysia, 81310 Skudai, Johor, Malaysia

Keywords: *Delta-Winged UAV, propeller locations, Aerodynamic Characteristics*

Abstract

The flow above delta wing is complicated and dominated by a very complex vortex structure. This study investigates the effects of propeller locations on the aerodynamic characteristics above a 55° sharp-edged non-slender delta wing UAV model. The experiments were conducted in a closed circuit UTM-LST wind tunnel at speeds of 20 and 25 m/s. In this project the propeller is located at three different locations namely; front, middle and rear. The result obtained from this experiment was compared with the clean wing configuration. The effects of propeller locations, angle of attack, Reynolds number and propeller advance ratio on the aerodynamic characteristics of this generic UAV model are discussed in this paper. The experimental data highlights an impact of propeller locations on lift, drag, moment and vortex system of the UAV. The results also showed that the propeller advance ratio, J influence the vortex system above UAV wing.

1 Introduction

Development of UAV was prompted by the manned aircrafts limitations [1]. As there are limitations for the piloted aircraft, application of the UAV in civil purposed has increased. The UAV is widely used in various applications such as in agriculture, map building, traffic surveillance, construction, film industry, safe and rescue mission and weather forecasting.

Delta wing UAVs generate more lift compared to the conventional design [2]. Delta wing UAVs produced strong vortex flow on its upper surface. The primary vortex developed on

the upper surface increases the wing lift in non-linear manner [3]. This makes delta wing is favourable in lift generation compared to the conventional wings.

Propeller is the best propulsion system for fixed-wing UAV [2]. Commonly, fixed-wing UAV is driven by either tractor or pusher propeller. Both tractor and pusher have their respective advantages and disadvantages [4][5]. In 2004, Galiński et al. have placed the propeller in the middle part of UAV to overcome the limitations of tractor and pusher configurations. Therefore, this project has emphasized on the wind tunnel experiment of the UAV model with three different propeller positions; namely front, middle and rear.

2 Wind tunnel experiments

The model has been designed to place the propeller at three different locations, i.e. front, middle and rear. Fig 1 (a-d) shows the generic delta-winged UAV model tested in this project. The model has been manufactured using aluminium has an overall length of 0.99 meter and overall width of 1.062 meter. To measure the surface pressure, 102 pressure points were placed on the upper surface of the wing. The location of pressure taps is shown in Fig 1e. This model has been designed based on several previous delta winged UAVs [1][2][4].

The experiments were conducted in 1.5m×2.0m×6m UTM-LST wind tunnel. The installation of the UAV model is shown in Fig 2 a & b. The tests were carried out at speeds of 20 and 25 m/s that corresponding to Reynolds number of 0.6×10^6 and 0.8×10^6 based on the mean aerodynamic chord (MAC) of the wing

model. EMAX brushless out-runner motor has been chosen to run the propeller. During the experiments, the propeller speed was controlled by a servo controller, which both instruments were connected each other. The system was powered using DC power supplied unit. For this project, the propeller speed was set at 6000 RPM for all test cases. In this experiment, two measurement techniques were employed on the wing. For first experiment, the steady balance data were recorded for all test conditions. The model is mounted to 6 axis balance measurement system located underneath the test section; this is shown in Fig 2c. For the last experiments, intensive surface pressure measurements were captured using UTM-LST pressure scanner.

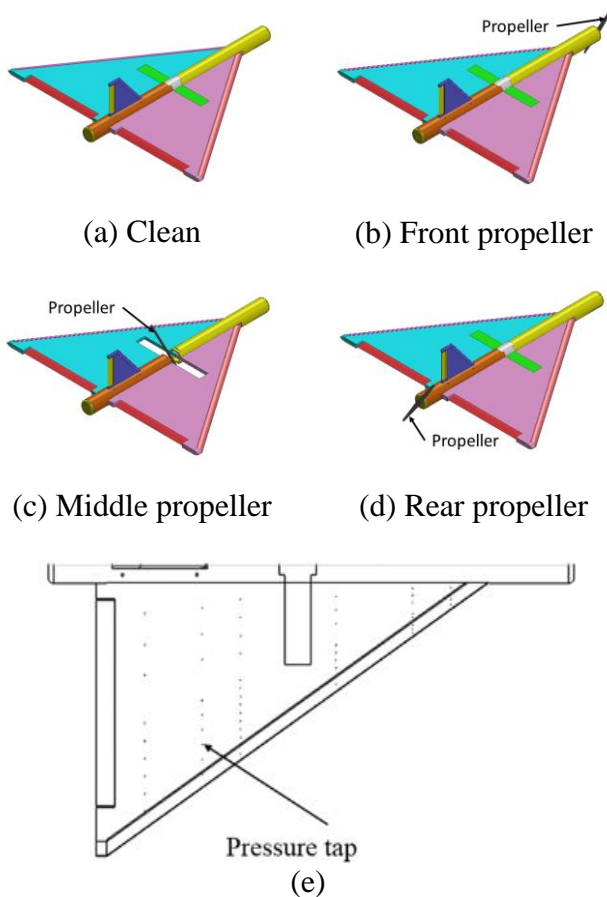


Fig.1 Test configurations

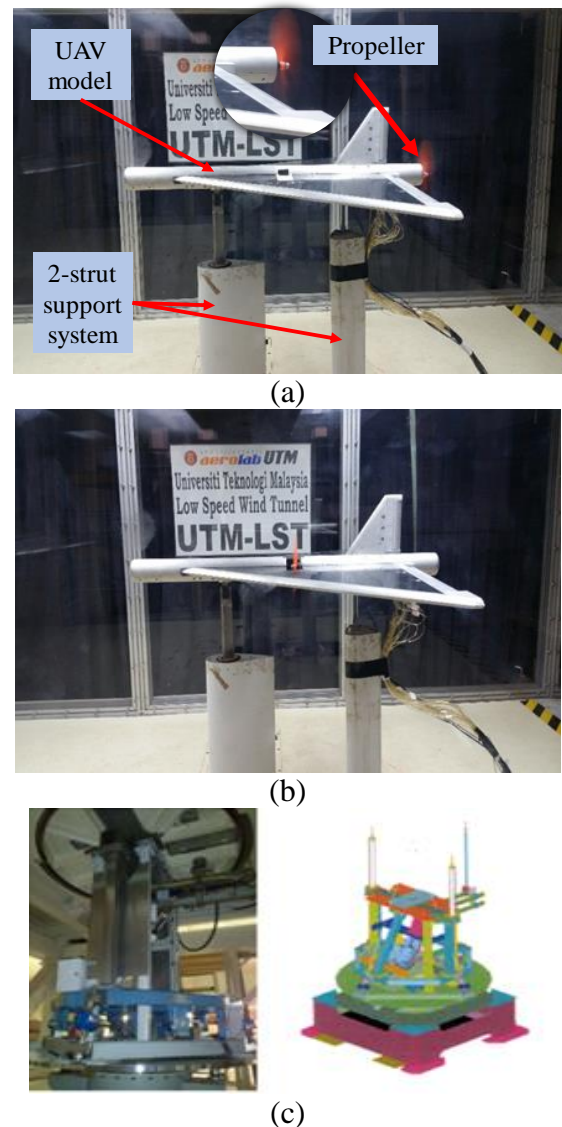


Fig.2 Installation of UAV model in UTM-LST

3 Results and discussion

3.1 Steady data

3.1.1 Effects of Reynolds number (Clean configuration)

Fig 3 shows the effects of Reynolds number on the steady balance data for the clean wing configuration. The $C_L-\alpha$ plot shows that the lift coefficient increases to about 1-4% when the Reynolds number is increased from 0.6 million to 0.8 million. The $C_D-\alpha$ plot shows that the drag coefficient is not affected by the Reynolds number. At a higher angle of attack, the gradient of the $C_M-\alpha$ curve decreases if the Reynolds number is increased. The effects of the

Reynolds number on the balance data are relatively small. This may be related to the vortex burst occurred on the wing[6].

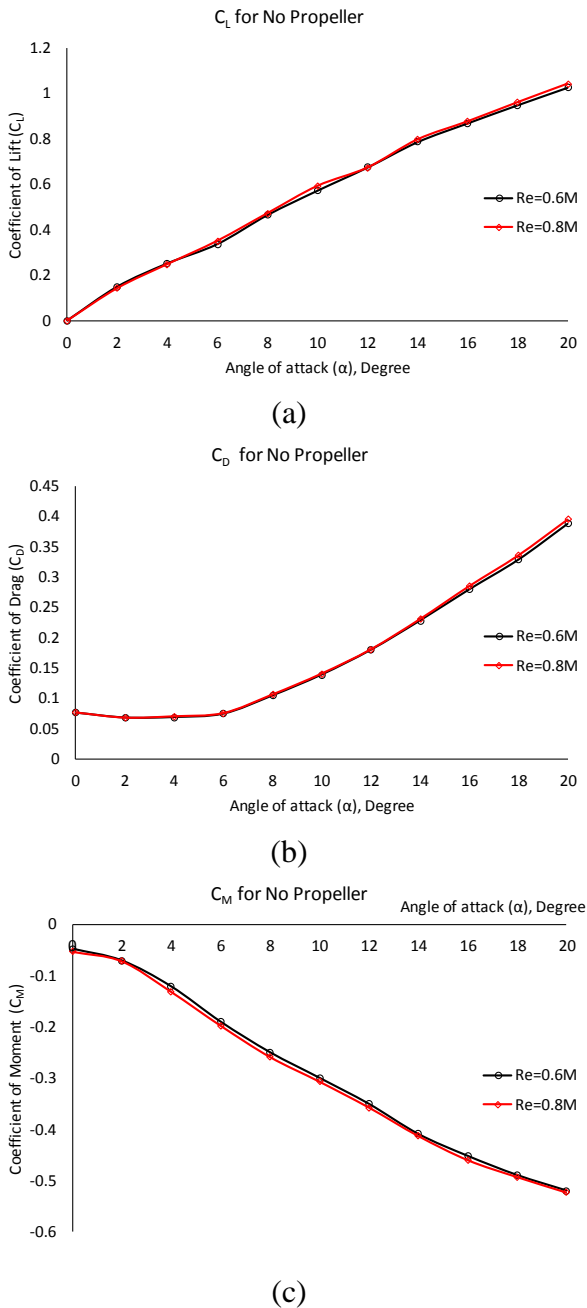


Fig.3 Effects of Reynolds number for clean configuration

3.1.2 Effects of propeller locations

The effects of propeller locations on lift, drag and moment coefficients are shown in Fig 4. From the figure, there are obvious differences between the data at constant Reynolds number. Generally, lift coefficient increases if the propeller is installed on the model. These results

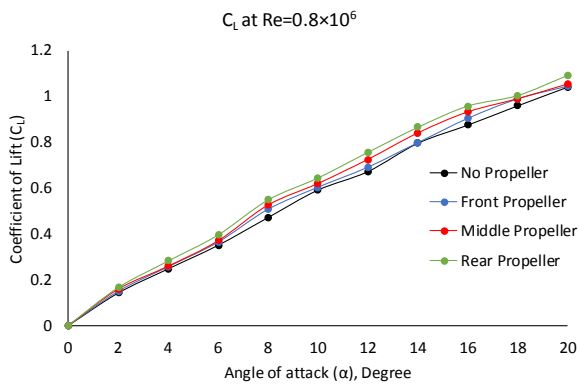
can be linked with the increases in the magnitude of the primary vortex compared to clean wing configuration. From the $C_L - \alpha$ plot, the highest lift is recorded when the propeller is installed at the rear position. At $\alpha=0$ to 6° , only slight differences in lift coefficients can be observed. After $\alpha=6^\circ$, the middle and rear propeller location has an obvious improvement on lift coefficient. At higher angle of attack, $\alpha \geq 18^\circ$, the lift decreasing for all propeller locations. This is because the vortex generated by the leading edge has become dominant.

The drag coefficient plot in Fig 4b shows that drag coefficients is increased if the propeller is installed. This showed that higher drag is induced at higher lift. From the observation, the middle propeller configuration has recorded the highest drag coefficient. Higher drag recorded by middle propeller is mainly due to the body-slot located in the middle part of the wing. The effects of body slot on the UAV model has been discussed by Galiński [7].

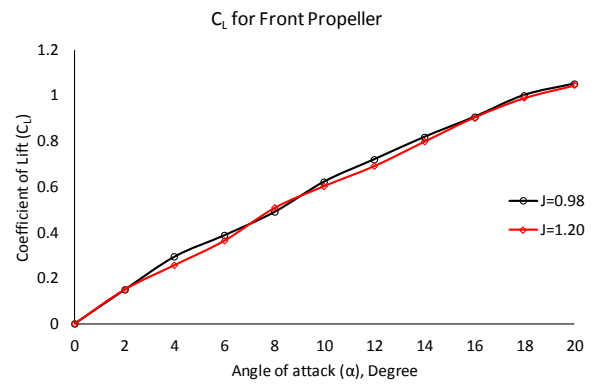
The pitching moment characteristic is shown in Fig 3c. Front propeller exhibits lower nose down pitching moment values. This observation may suggest that accelerated flow from the propeller can increase the size of the primary vortex in the apex region. The front propeller has pressurized the flow in the leading area and creating the pitching-up moment on the model [4]. For the rear and middle propeller configurations, the moment coefficient is increased at higher angle of attack. This suggests that greater primary vortex developed when the propeller is installed. The hypothesis made in this section will be supplemented by the surface pressure measurement data.

3.1.3 Effects of advance ratio, J (Propeller configurations)

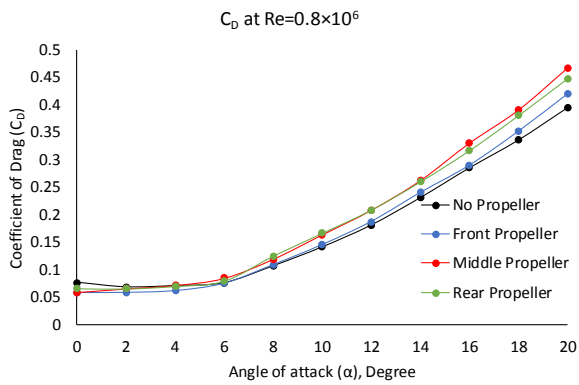
Fig 5 discusses the effects of the propeller advance ratio, J. For this paper only the data at front location is discussed. It can be observed that all coefficients are greater when the value of J is lower. As the value of J is increased, the effects of the free stream become more dominant compared to the propeller flow.



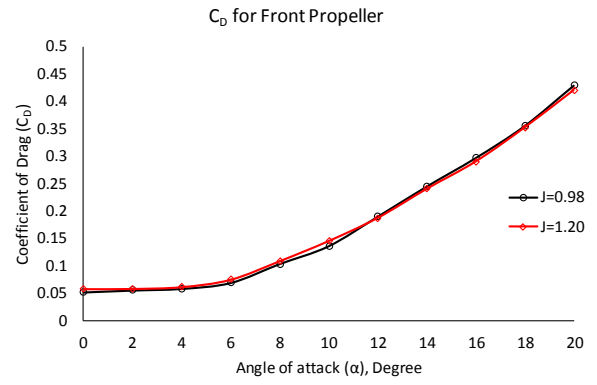
(a)



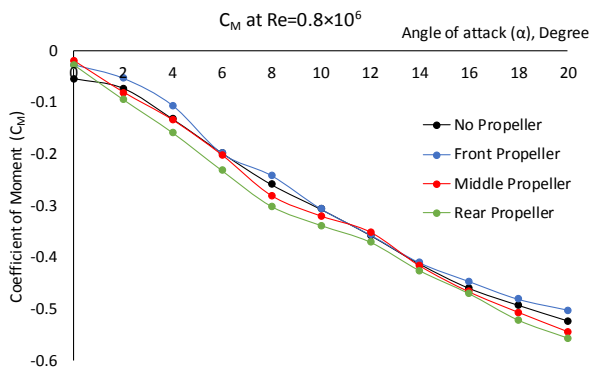
(a)



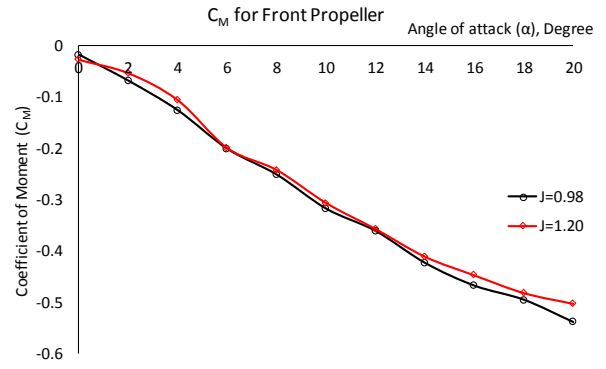
(b)



(b)



(c)



(c)

Fig.4 Effects of propeller locations on lift, drag and moment coefficient

Fig.5 Effects of advance ratio on balance data

3.2 Surface pressure measurement

3.2.1 Effects of Reynolds number

This section discussed the surface pressure measurement obtained on the upper surface of the wing. Fig 6 shows the effects of Reynolds number on surface pressure measurement for the clean wing at $\alpha=12^\circ$. From the plot it can be observed that the pressure distribution above the wing has a small effect if the Reynolds number is increased. The data showed a small changed

in vortex trajectory, this happened because the flow already reached the asymptote state [8]. The results contrast with the previous publications (Ol & Gursul [9][10]) who showed that the vortex breakdown is promoted if the Reynolds number is increased on non-slender delta wing. The results obtained here in UTM may suggest that at higher Reynolds number, the vortex structure above non-slender delta wing is similar to slender delta wing flow topology. More experiments are needed to confirm this hypothesis.

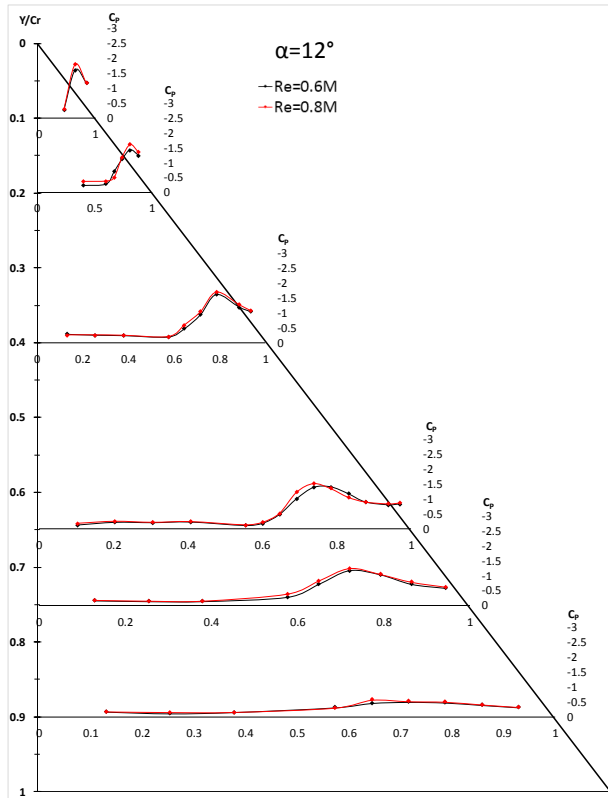


Fig.6 Effects of Reynolds number on pressure distribution

3.2.3 Effects of advance ratio, J

The effects of the advance ratio on the vortex system are shown in Fig 7. For this paper only the data at front and middle locations are discussed. It can be observed that the installation of propeller has significant effects on the data for all test cases. By increasing the advance ratio, the suction peak of the primary vortex is reduced. This is because the effects of free stream velocity have become dominant compared to the energy induced by the propeller. The vortex enhancement is increases when the propeller speed is increased [14][15]. The increase in vortex strength at lower J is consistent with the increase of lift and drag coefficients.

3.2.1 Effects of propeller locations

The effects of propeller locations on the vortex system above the wing are shown in Figs 8, 9 and 10. The primary vortex starts to develop in at the apex region for all wing configurations. The sharpness of the wing caused the primary

vortex is developed in this case [11-13]. Fig 8 discussed the vortex system if the propeller is located in front position. It can be noticed that the size of the primary vortex is increased. The size of the primary vortex is increased significantly for the first three pressure taps locations, i.e. $Y/Cr=0.1, 0.2, 0.4$. Downstream from the apex, no changes were observed. This suggests that the additional momentum toward the vortex structure incapable to maintain vortex consistency. The accelerated flow from the propeller has pushed the vortex toward the leading edge of the wing.

The effects of vortex properties if the propeller is been place around the middle of the model are discussed in Fig 9. At this position, the primary vortex is developed in the apex region. The size of the primary vortex is increased in the region behind the propeller. In the region near to the apex or at $Y/Cr=0.1, 0.2, 0.4$, the primary vortex core is located at slightly inboard of the wing; this is because the propeller has created a suction effect to the vortex system. Further aft from the propeller, the primary vortex is pushed slightly towards the leading edge. This can be seen in the surface pressure plots at $Y/Cr=0.65, 0.75$ and 0.9 . More experiments are needed to verify this.

Fig 10 presents the effects on the vortex system if the propeller is positioned in the rear region. The results show that primary vortex is bigger starting from the apex of the wing. In downstream region, higher suction peak is developed and this is consistent with the previous researches (Ji et al. & Traub[14][15]). The downstream suction created by the rear propeller pulled the vortex core slightly inboard of the wing.

In general, the propeller has increased the absolute value of pressure coefficient and improves the vortex strength. The propeller has accelerated the flow above and lower pressure region is created on the wing. However, the development of the vortex is not able to prevent the formation of vortex breakdown at a higher angle of attack. Taken example at $\alpha=16^\circ$ and 20° , the vortex breakdown is observed at $Y/Cr=0.65$ for all propeller configurations. In the trailing edge region ($Y/Cr=0.9$), the

influence of the propeller is diminished by the vortex breakdown.

4 Conclusions

The results presented in this paper show that the installation of the propeller has influenced the lift, drag and moment coefficients. It is found that the propeller advance ratio plays important roles in the development of primary vortex above delta-winged model. Higher value of J has reduced the influence of the vortex on the wing.

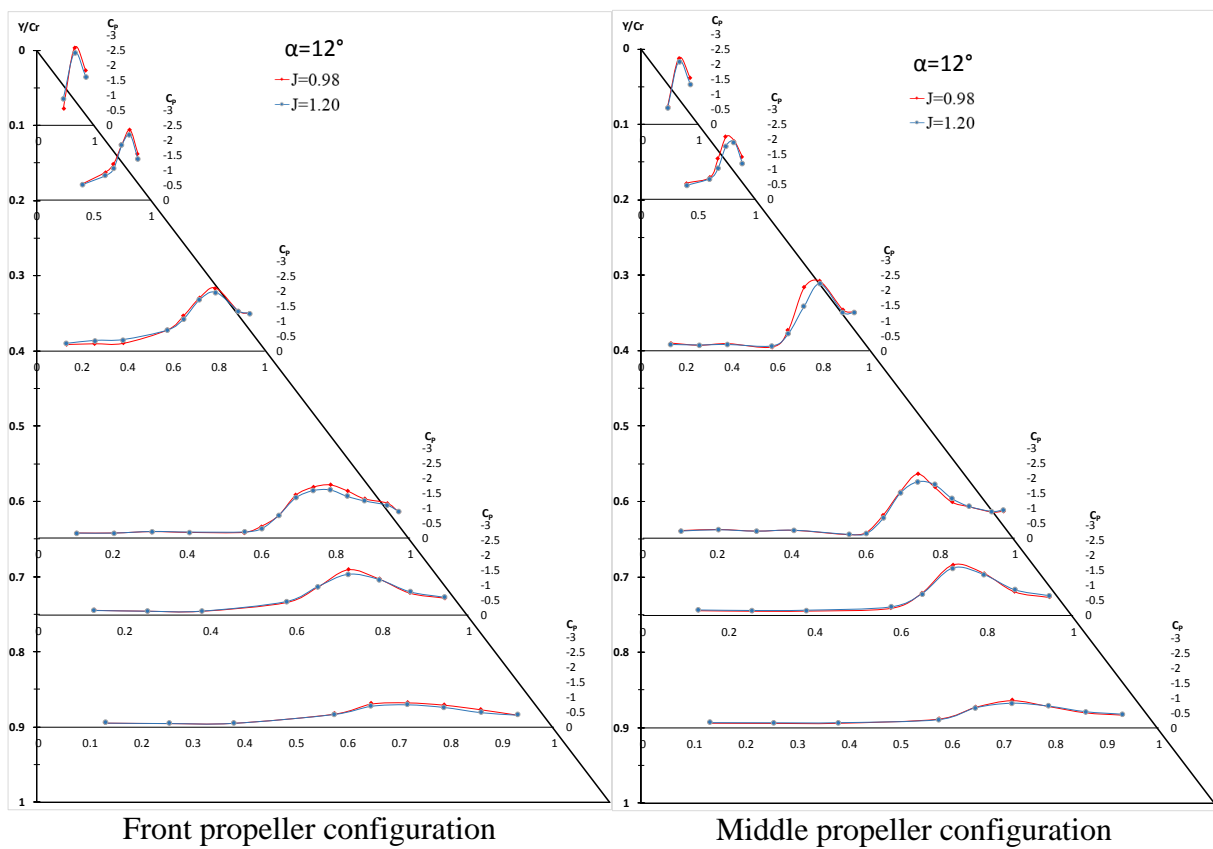


Fig.7 Advance ratio effects on pressure distribution

EFFECTS OF PROPELLER LOCATIONS ON THE VORTEX SYSTEM ABOVE DELTA-SHAPED UAV MODEL

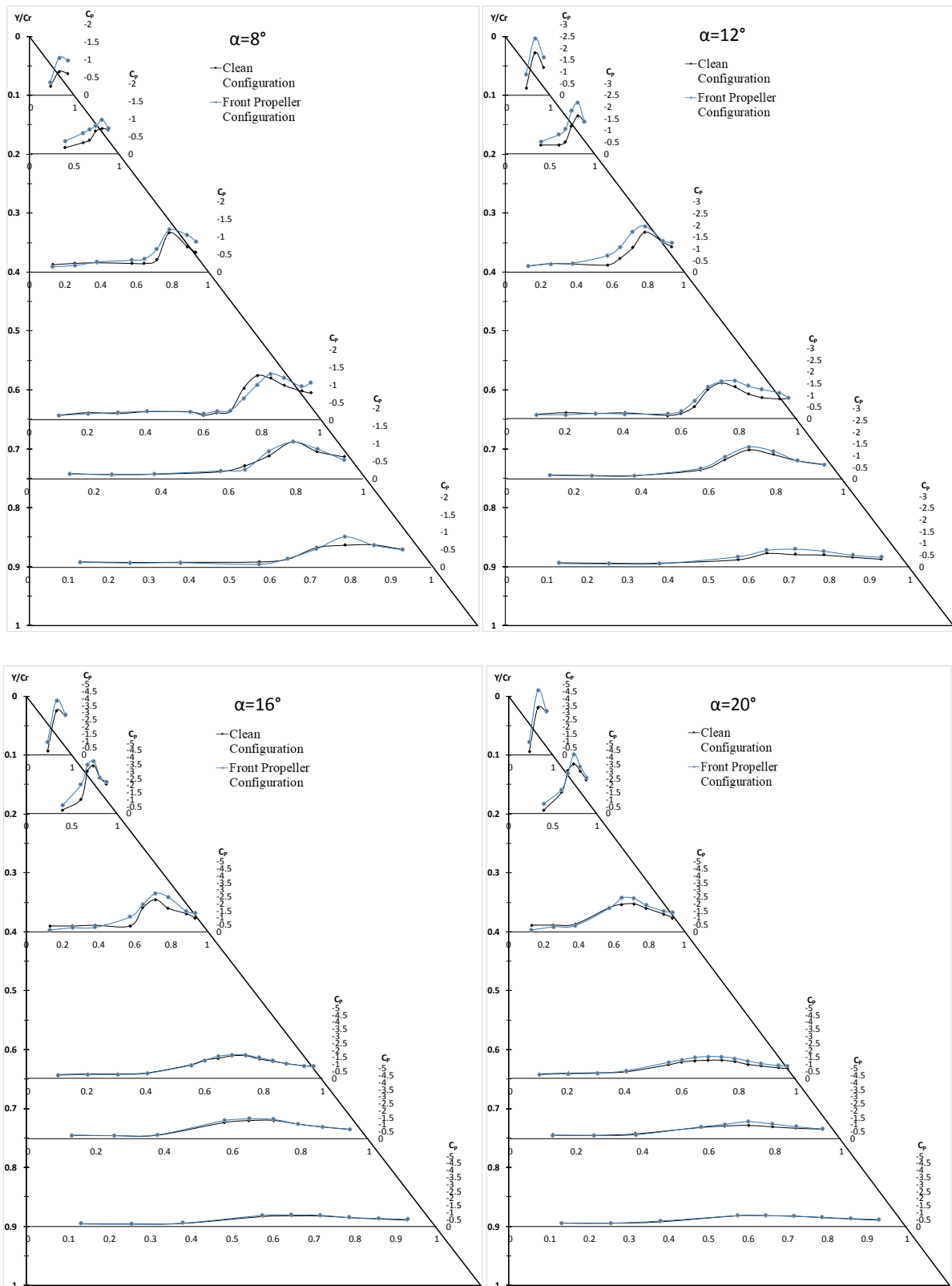


Fig.8 The effects of front propeller on vortex properties

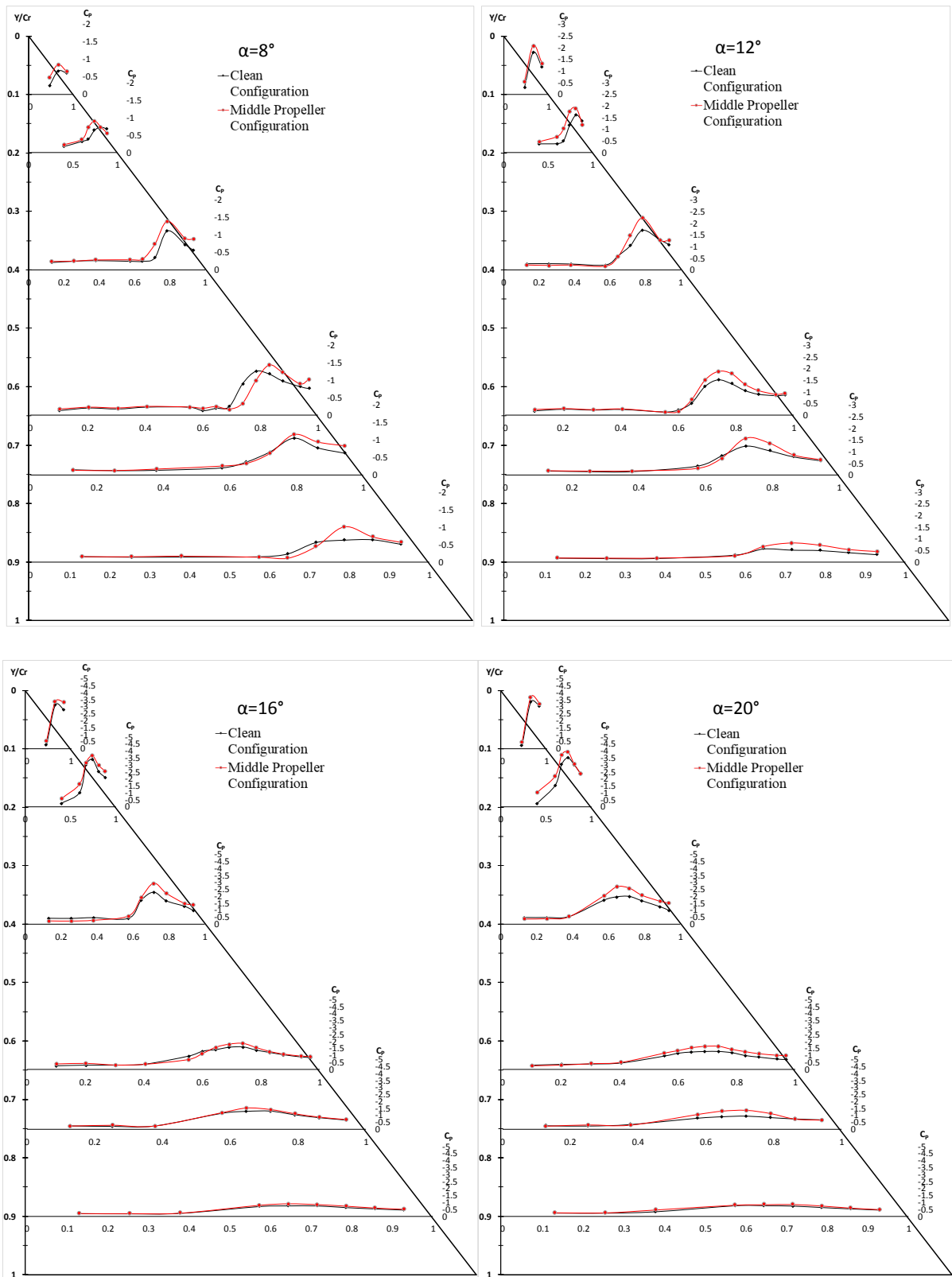


Fig.9 The effects of middle propeller on vortex properties

EFFECTS OF PROPELLER LOCATIONS ON THE VORTEX SYSTEM ABOVE DELTA-SHAPED UAV MODEL

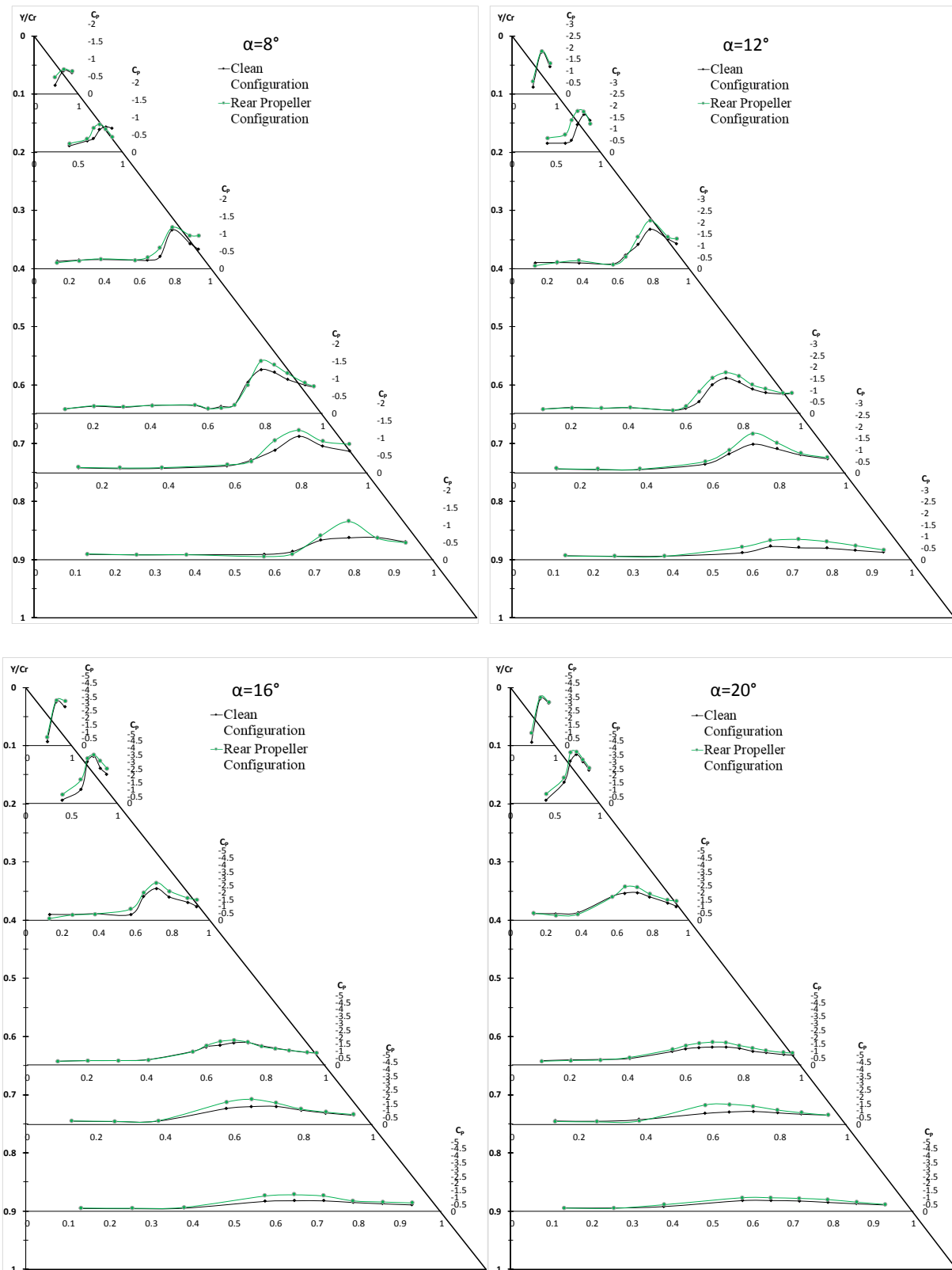


Fig.10 the effects of rear propeller on vortex properties

References

- [1] Koma AY, Afshar S, Maleki H, Mohammadshahi D and Shahi H. Design and fabrication of delta wing shape MAV. *10th WSEAS International Conference on Automatic Control, Modelling & Simulation*, Istanbul, Turkey, pp 267-274, 2008.
- [2] Galiński C, Lawson NJ and Żbikowski R. Delta Wing with Leading Edge Extension and Propeller Propulsion for Fixed Wing MAV. *24th International Congress of the Aeronautical Sciences*, 29 August – 3 September, Yokohama, Japan, 2004.
- [3] Polhamus EC. A concept of the vortex lift of sharp-edge delta wings based on a leading-edge-suction analogy. *NASA Technical Note D-3767*, 1966
- [4] Ahn J and Lee D. Aerodynamic Characteristics of a Micro Air Vehicle and the Influence of Propeller Location. *31st AIAA Applied Aerodynamics Conference*, 24-27 June, San Diego, CA, AIAA2013-2655, 2013.
- [5] Mieloszyk J and Galiński C. Assessment of the concept of a propeller working in a slot in the middle of wing of a micro air vehicle. *Archive of Mechanical Engineering*, Vol. 60, No. 2, pp 269-282, 2013.
- [6] Verhaagen NG. Effects of Leading-Edge Radius on Aerodynamic Characteristics of 50° Delta Wings. *48th AIAA Aerospace Sciences Meeting Including the New Horizons Forum and Aerospace Exposition*. 4-7 January, Orlando, Florida, AIAA 2010-323, 2010.
- [7] Galiński C and Mieloszyk J. Results of the Gust Resistance MAV Programme. *28th International Congress of the Aeronautical Sciences*, 23-28 September, Brisbane, Australia, 2012.
- [8] Gursul I, Gordnier R and Visbal M. Unsteady Aerodynamics of Non-slender Delta Wings. *Progress in Aerospace Sciences*, Vol. 41, No. 7, pp 515-557, 2005.
- [9] Ol MV and Gharib M. Leading-Edge Vortex Structure of Non-slender Delta Wings at Low Reynolds Number. *AIAA Journal*, Vol. 41, No. 1, pp 16-26, 2003.
- [10] Taylor GS, Schnorbus T and Gursul I. An Investigation of Vortex Flows Over Low Sweep Delta Wings. *33rd AIAA Fluid Dynamics Conference and Exhibit*, 23-26 June, Orlando, Florida, AIAA 2003-4021, 2003.
- [11] Hummel D. Effects of Boundary Layer Formation on the Vortical Flow Above Slender Delta Wings. *RTO specialist Meeting on Enhancement of NATO military Flight Vehicle Performance by Management of Interacting Boundary Layer transition and Separation*. Meeting Proceedings RTO-MPAVT-111. pp 30-1 to 30-2, 2004.
- [12] Luckring JM. Reynolds Number, Compressibility, and Leading Edge Bluntness Effects on Delta Wing Aerodynamics. *24th International Congress of the Aeronautical Sciences*. 29 August – 3 September. Yokohama, Japan, 2004.
- [13] Said M, Mat S, Mansor S, Abdul-Latif A, Lazim TM. Reynolds Number Effects on Flow Topology Above Blunt-Edge Delta Wing VFE-2 Configurations. *53rd AIAA Aerospace Sciences Meeting*, 5 - 9 January, Kissimmee, Florida, AIAA 2015-1229, 2015.
- [14] Ji Z, Marchetta J, Hochstein J and Mo JD. The Effect of Downstream Suction on the Delta Wing Leading-Edge Vortex. *Proceedings of the Eight Asian Congress of Fluid Mechanics*, 6-10 December, Shenzhen, China, pp 382-387, 1999.
- [15] Traub LW. Effect of a Pusher Propeller on a Delta Wing. *Aerospace Science and Technology*, Vol. 41, No. 12, pp 115-121, 2016.

Contact Author Email Address

The contact author email address, mail to:

khushairi749@gmail.com &
shabudin@fkm.utm.my, shah@mail.fkm.utm.my,
mazuriah.said@gmail.com

Copyright Statement

The authors confirm that they, and/or their company or organization, hold copyright on all of the original material included in this paper. The authors also confirm that they have obtained permission, from the copyright holder of any third party material included in this paper, to publish it as part of their paper. The authors confirm that they give permission, or have obtained permission from the copyright holder of this paper, for the publication and distribution of this paper as part of the ICAS 2016 proceedings or as individual off-prints from the proceedings.